

Supplement of *Clim. Past*, 15, 1113–1131, 2019
<https://doi.org/10.5194/cp-15-1113-2019-supplement>
© Author(s) 2019. This work is distributed under
the Creative Commons Attribution 4.0 License.



Supplement of

Early summer hydroclimatic signals are captured well by tree-ring earlywood width in the eastern Qinling Mountains, central China

Yesi Zhao et al.

Correspondence to: Jiangfeng Shi (shijf@nju.edu.cn)

The copyright of individual parts of the supplement might differ from the CC BY 4.0 License.

Table S1. Correlation coefficients between the tree-ring width chronologies from the two study sites, Baiyunshan and Longchiman, over their common period 1850–2005.

Chronologies	Detrending method		
	NELR	SP67	SPA50
EWV STD	0.63 / 0.59	0.64 / 0.60	0.62 / 0.57
LWW STD	0.40 / 0.51	0.46 / 0.49	0.46 / 0.47
TRW STD	0.58 / 0.58	0.60 / 0.62	0.61 / 0.63
EWV SSF	0.64 / 0.60	0.57 / 0.53	0.55 / 0.49
LWW SSF	0.43 / 0.54	0.37 / 0.51	0.35 / 0.47
TRW SSF	0.57 / 0.57	0.50 / 0.54	0.50 / 0.54

Note: The correlation coefficients before (after) the slashes are for the original (prewhitened and linearly detrended) STD and SSF chronologies. All correlation coefficients are statistically significant at the 0.001 level based on Monte Carlo test (Efron and Tibshirani, 1986; Macias-Fauria et al., 2012).

Table S2. Descriptive statistics of the composite STD and SSF tree–ring width chronologies when EPS ≥ 0.85 .

Detrending method	Chronology	Starting year when EPS ≥ 0.85	Standard deviation	Mean sensitivity	First-order autocorrelation
NELR	EWV STD	1868	0.238	0.225	0.348
	LWW STD	1877	0.25	0.221	0.421
	TRW STD	1871	0.221	0.200	0.458
SP67	EWV STD	1871	0.235	0.222	0.354
	LWW STD	1877	0.247	0.227	0.38
	TRW STD	1871	0.218	0.200	0.439
SPA50	EWV STD	1867	0.234	0.223	0.328
	LWW STD	1875	0.245	0.225	0.384
	TRW STD	1866	0.215	0.200	0.42
NELR	EWV SSF	1868	0.245	0.226	0.382
	LWW SSF	1875	0.263	0.221	0.451
	TRW SSF	1868	0.227	0.200	0.479
SP67	EWV SSF	1868	0.245	0.225	0.397
	LWW SSF	1875	0.255	0.226	0.404
	TRW SSF	1871	0.227	0.201	0.48
SPA50	EWV SSF	1867	0.234	0.207	0.418
	LWW SSF	1875	0.246	0.214	0.426
	TRW SSF	1866	0.214	0.191	0.459

Note: All statistics were calculated using the R package “dplr” version 1.6.9 (Bunn et al., 2018).

Table S3. Statistics of the detrended ring-width series over their common period 1915–2005.

Detrending method	Chronology	Var_{pc1}	Rbar_{eff}	SNR	EPS
NELR	EWV STD	0.386	0.443	25.878	0.963
	LWW STD	0.328	0.358	18.175	0.948
	TRW STD	0.384	0.433	24.806	0.961
SP67	EWV STD	0.427	0.492	31.452	0.969
	LWW STD	0.353	0.400	21.702	0.956
	TRW STD	0.422	0.481	30.104	0.96
SPA50	EWV STD	0.411	0.471	29.007	0.967
	LWW STD	0.341	0.384	20.315	0.953
	TRW STD	0.404	0.459	27.607	0.965
NELR	EWV SSF	0.399	0.456	27.291	0.965
	LWW SSF	0.317	0.346	17.252	0.945
	TRW SSF	0.393	0.439	25.492	0.962
SP67	EWV SSF	0.453	0.520	35.298	0.972
	LWW SSF	0.366	0.417	23.308	0.959
	TRW SSF	0.441	0.504	33.033	0.971
SPA50	EWV SSF	0.474	0.539	37.994	0.974
	LWW SSF	0.352	0.399	21.627	0.956
	TRW SSF	0.431	0.491	31.354	0.969

Note: The common period for the tree-ring width dataset was calculated with the “common.interval” function in R package “dplR” version 1.6.9 (Bunn et al., 2018) based on a trade-off between the maximum number of series and years. The statistics, Var_{pc1} , Rbar_{eff} , SNR, and EPS represent the variance explained by the first eigenvector, effective chronology signal, signal-to-noise ratio, and expressed population signal, respectively. The Var_{pc1} was calculated using the Program ARSTAN40c (Cook and Krusic, 2006), and the other statistics were calculated using the R package “dplR” version 1.6.9 (Bunn et al., 2018).

Table S4. The meteorological stations utilized by CRU dataset (<http://www.cru.uea.ac.uk/data>) located in the area between latitudes 32° N and 34.5° N, and longitudes 111° E and 112° E.

Meteorological station	Longitude (°E)	Latitude (°N)	Climatic factor	Temporal cover
Lushi	111.03	34.05	Precipitation	1952.07–2013.12
			Temperature	1952.07–2016.12
Laohekou	111.73	32.43	Precipitation	1933.02–1933.11; 1934.01–1935.06; 1935.08–1935.12; 1936.08–1938.07; 1950.06–2005.06; 2005.08–2013.12
			Temperature	1951.01–2016.12
Yunxian	111.8	32.9	Precipitation	1933.03–1938.05; 1938.07–1947.10; 1950.03–1990.12; 1991.05; 1991.07–1991.08

Table S5. The reconstructed May–July (MJJ) scPDSI during the period 1868–2005.

Year	scPDSI	Year	scPDSI	Year	scPDSI	Year	scPDSI
1868	-1.427	1904	1.167	1940	-1.139	1976	-1.394
1869	2.307	1905	2.260	1941	-1.300	1977	-1.474
1870	-0.388	1906	3.654	1942	0.859	1978	-1.829
1871	-0.321	1907	-0.630	1943	1.046	1979	-0.046
1872	-0.227	1908	-0.080	1944	2.380	1980	2.065
1873	-0.918	1909	-0.777	1945	-0.656	1981	0.088
1874	-1.682	1910	2.045	1946	1.589	1982	0.859
1875	-1.374	1911	3.842	1947	0.986	1983	4.150
1876	0.564	1912	2.012	1948	2.809	1984	2.327
1877	-1.568	1913	-0.495	1949	2.950	1985	1.891
1878	0.570	1914	-0.006	1950	1.998	1986	-0.770
1879	-3.612	1915	0.939	1951	1.428	1987	1.851
1880	-1.984	1916	-0.636	1952	1.549	1988	-0.127
1881	-0.991	1917	-1.179	1953	1.160	1989	0.269
1882	1.958	1918	-0.710	1954	1.355	1990	2.320
1883	2.622	1919	-0.167	1955	-1.682	1991	1.194
1884	1.254	1920	-1.749	1956	1.415	1992	-0.991
1885	3.071	1921	0.497	1957	0.356	1993	1.288
1886	1.522	1922	0.758	1958	0.550	1994	-2.118
1887	1.321	1923	-2.279	1959	0.523	1995	-2.104
1888	0.624	1924	-1.072	1960	-0.107	1996	0.041
1889	1.254	1925	0.255	1961	-0.247	1997	-0.556
1890	0.624	1926	-2.325	1962	0.517	1998	1.341
1891	-1.441	1927	-0.341	1963	0.336	1999	0.115
1892	-0.743	1928	-1.782	1964	1.616	2000	-2.942
1893	1.462	1929	-2.527	1965	-0.241	2001	-1.963
1894	3.057	1930	1.931	1966	0.229	2002	0.289
1895	2.112	1931	1.495	1967	0.262	2003	0.624
1896	1.549	1932	-0.569	1968	-1.568	2004	0.517
1897	1.120	1933	2.514	1969	-0.878	2005	1.777
1898	3.768	1934	3.111	1970	1.355		
1899	-1.025	1935	0.523	1971	1.777		
1900	-2.238	1936	3.721	1972	0.839		
1901	-0.489	1937	0.423	1973	2.970		
1902	-1.923	1938	0.249	1974	1.428		
1903	0.544	1939	-1.018	1975	1.020		

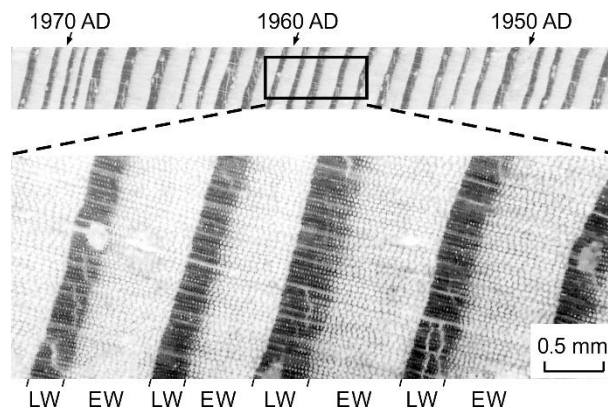


Figure S1. Photograph of a section of a *P. tabulaeformis* tree-ring sample (LCM0118A). The distinct earlywood (EW) and latewood (LW) segments can be identified by inspection under a microscope.

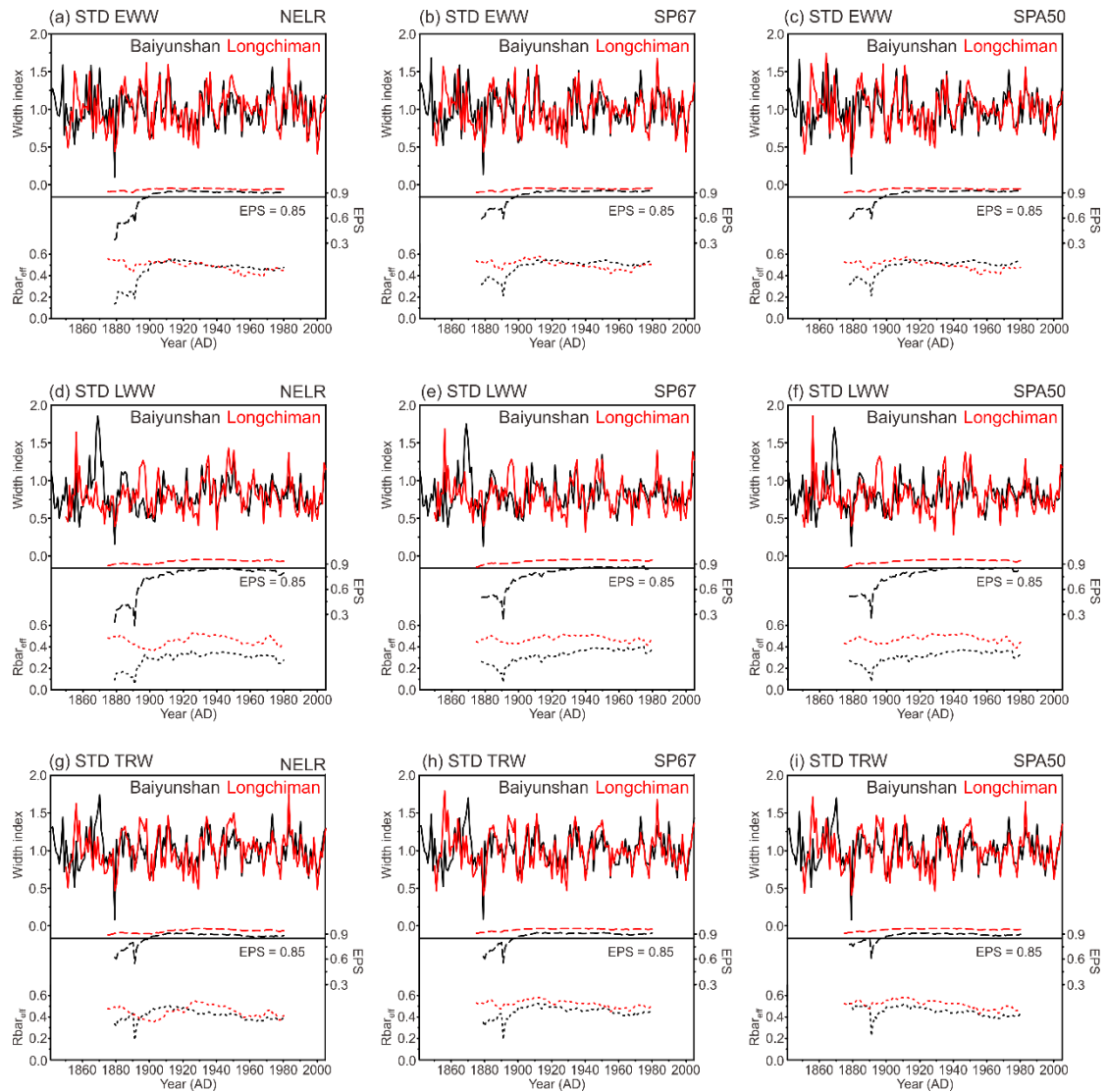


Figure S2. Standard (STD) tree-ring width chronologies (solid curves) generated using different detrending methods for (a–c) earlywood width (EWW), (d–f) latewood width (LWW), and (g–i) total tree–ring width (TRW) at the two study sites, Baiyunshan (black) and Longchiman (red). The detrending methods are: (1) negative exponential functions combined with linear regression with negative (or zero) slope (NELR), (2) cubic smoothing splines with a 50 % frequency cutoff at 67 % of the series length (SP67), and (3) age-dependent splines with an initial stiffness of 50 years (SPA50). The dashed and dotted curves denote the running expressed population signal (EPS) and effective chronology signal ($Rbar_{eff}$), respectively. The horizontal line indicates the threshold EPS value of 0.85. The running EPS and $Rbar_{eff}$ values were calculated over a 51–year window.

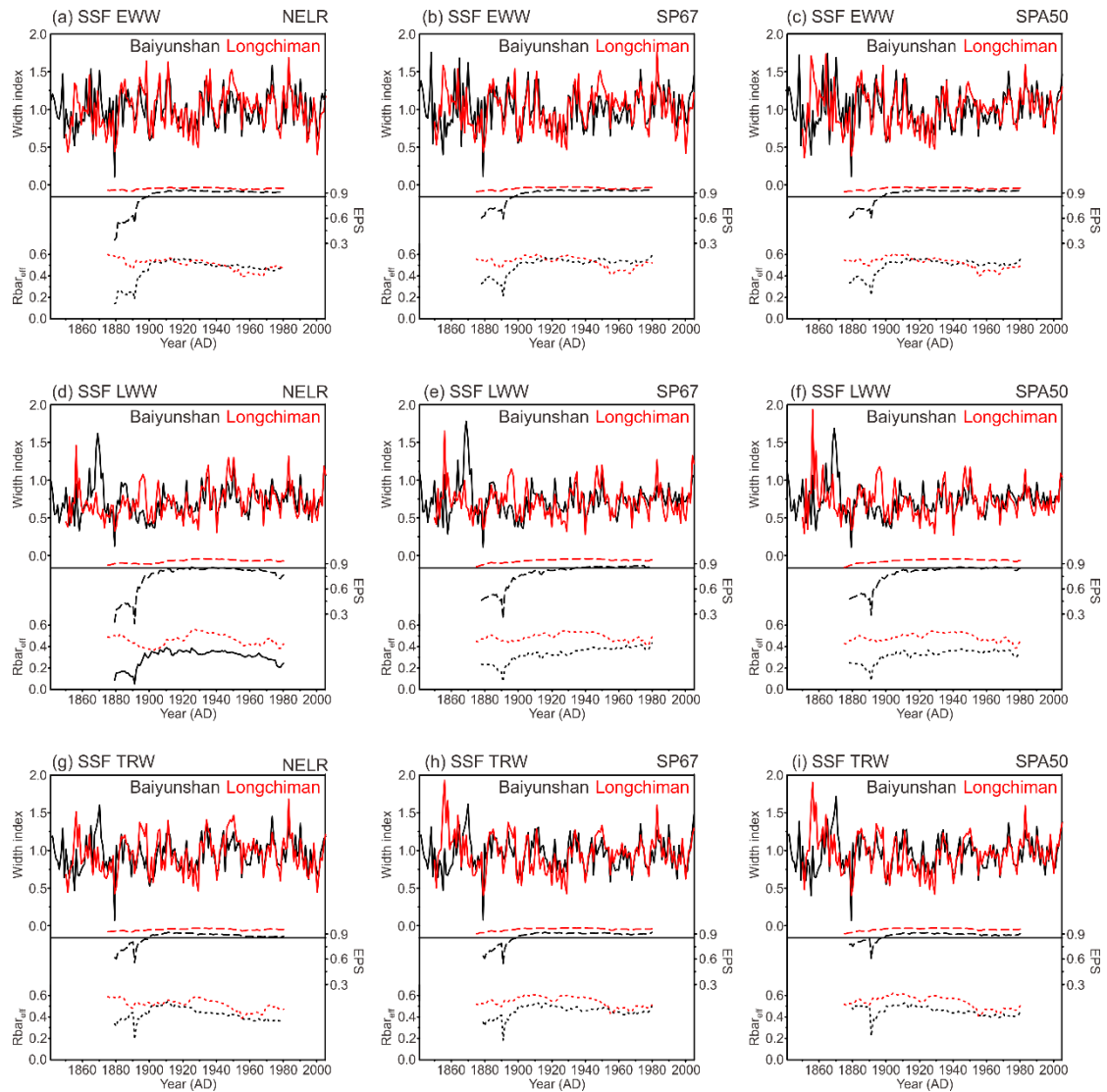


Figure S3. Signal-free (SSF) tree-ring width chronologies (solid curves) generated using different detrending methods for (a–c) earlywood width (EWW), (d–f) latewood width (LWW), and (g–i) total tree–ring width (TRW) at the two study sites, Baiyunshan (black) and Longchiman (red). The detrending methods are: (1) negative exponential functions combined with linear regression with negative (or zero) slope (NELR), (2) cubic smoothing splines with a 50 % frequency cutoff at 67 % of the series length (SP67), and (3) age-dependent splines with an initial stiffness of 50 years (SPA50). The dashed and dotted curves denote the running expressed population signal (EPS) and effective chronology signal ($Rbar_{eff}$), respectively. The horizontal line indicates the threshold EPS value of 0.85. The running EPS and $Rbar_{eff}$ values were calculated over a 51–year window.

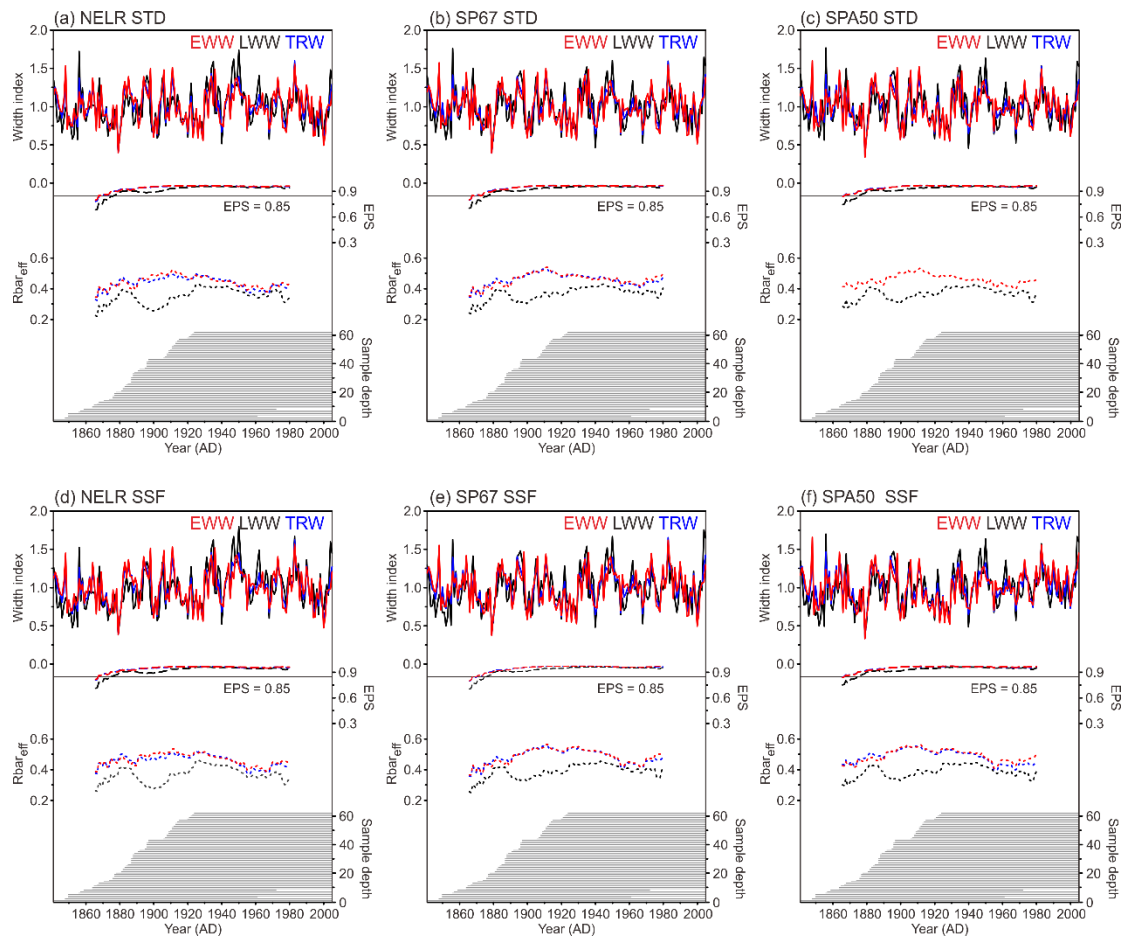


Figure S4. Composite (a–c) STD and (d–f) SSF tree-ring width chronologies for EWW (red), LWW (black), and TRW (blue) generated using the merged tree-ring samples from the two study sites, Baiyunshan and Longchiman, based on different detrending methods. The detrending methods are: (1) negative exponential functions combined with linear regression with negative (or zero) slope (NELR), (2) cubic smoothing splines with a 50 % frequency cutoff at 67 % of the series length (SP67), and (3) age-dependent splines with an initial stiffness of 50 years (SPA50). The dashed and dotted curves denote the running expressed population signal (EPS) and effective chronology signal ($Rbar_{eff}$), respectively. The horizontal line indicates the threshold EPS value of 0.85. The running EPS and $Rbar_{eff}$ values were calculated over a 51-year window. The segment plot indicates the sample depth (core).

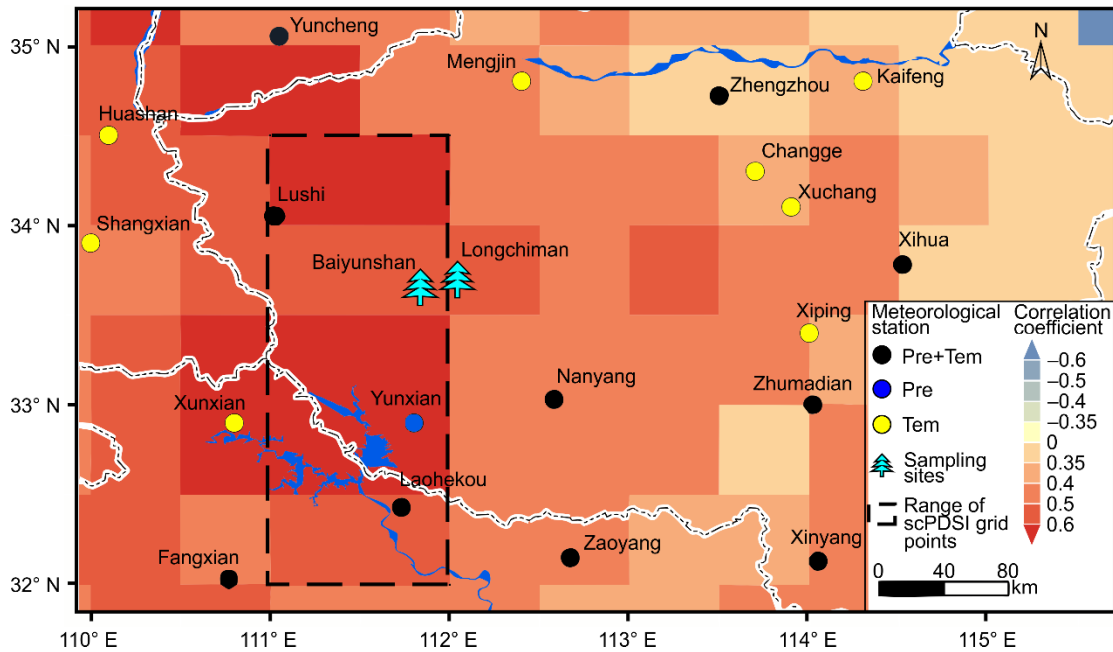


Figure S5. Spatial distribution of the meteorological stations included in the CRU dataset (<http://www.cru.uea.ac.uk/data>) around the tree-ring sampling sites, Baiyunshan and Longchiman. Black cycles represent the meteorological stations that provide both precipitation and temperature data. While, Blue (yellow) cycles represent those that only provide precipitation (temperature) data. The dashed rectangle indicates the range of scPDSI grid points used for calibration in this study. The color patches denote the spatial correlation coefficients between May-July scPDSI and NELR based EWW STD chronology.

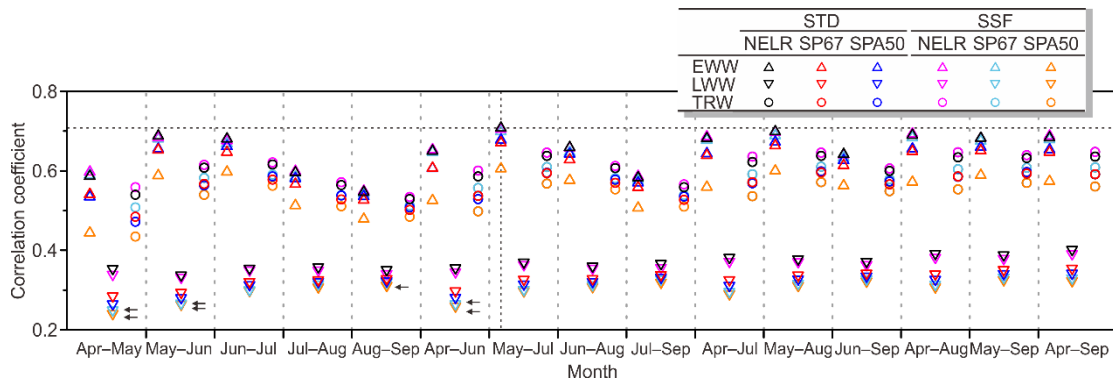


Figure S6. Correlation coefficients between the tree-ring width chronologies and multi-month averaged scPDSI (April to September of the current year). Upward triangles, downward triangles, and circles indicate the chronologies of EWW, LWW, and TRW, respectively. The color black, red and blue indicate the STD chronologies generated using the detrending methods NELR, SP67, and SPA50, while color magenta, cyan, and orange indicate the SSF chronologies generated using the detrending methods NELR, SP67, and SPA50, respectively. The arrow indicates that the corresponding correlation does not reach the 0.05 significance level, which was tested using the Monte Carlo method (Efron and Tibshirani, 1986; Macias-Fauria et al., 2012).

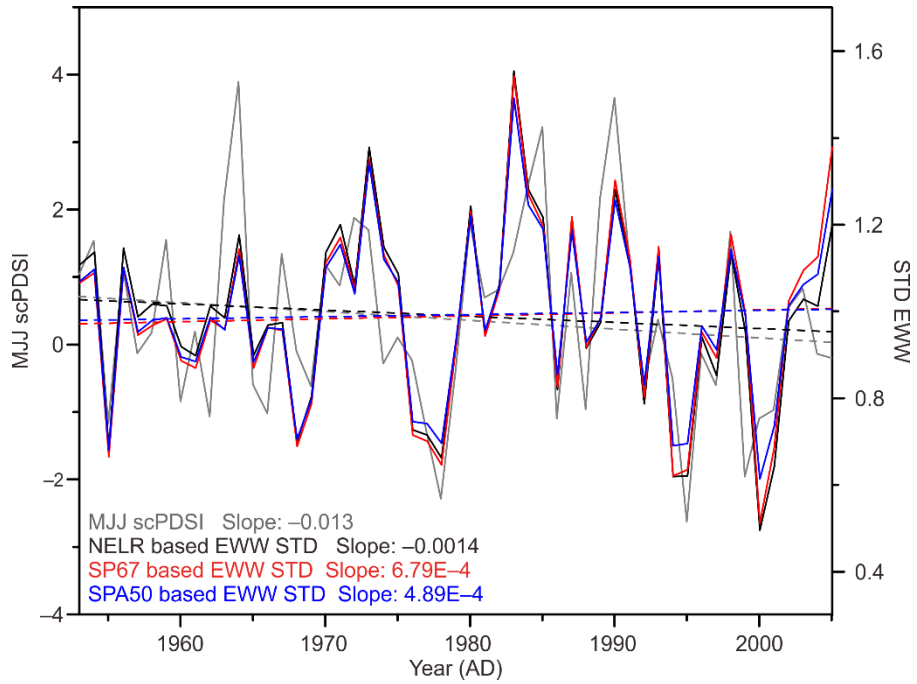


Figure S7. Comparisons between the MJJ scPDSI (gray) and EWW STD chronologies generated using the detrending methods NELR (black), SP67 (red), and SPA50 (blue) during the period 1953–2005. The dashed lines represent the linear trends. The slope coefficients are presented in the bottom left corner of the figure.

References

Bunn, A., Korpela, M., Biondi, F., Campelo, F., Mérian, P., Qeadan, F., Zang, C., Pucha-Cofrep, D., and Wernicke, J.: dplR: Dendrochronology Program Library in R, <https://CRAN.R-project.org/packages=dplR>, r package version 1.6.9, 2018.

Cook E.R., Krusic P.J.: ARSTAN 41: a tree-ring standardization program based on detrending and autoregressive time series modeling, with interactive graphics, Tree-Ring Laboratory, Lamont Doherty Earth Observatory of Columbia University, New York, 2006.

Efron, B., and Tibshirani, R.: Bootstrap methods for standard errors, confidence intervals, and other measures of statistical accuracy, *Stat. Sci.*, 1, 54–75, <https://www.jstor.org/stable/2245500>, 1986.

Macias-Fauria, M., Grinsted, A., Helama, S., and Holopainen, J.: Persistence matters: Estimation of the statistical significance of paleoclimatic reconstruction statistics from autocorrelated time series, *Dendrochronologia*, 30, 179–187, <https://doi.org/10.1016/j.dendro.2011.08.003>, 2012.